

The Global Cycles of Sulfur and Mercury

OUTLINE

Introduction	469	The Atmospheric Budget of Carbonyl Sulfide	480
The Global Sulfur Cycle	471	The Global Mercury Cycle	482
Temporal Perspectives on the Global Sulfur Cycle	475	Summary	485

INTRODUCTION

Sulfur is found in valence states ranging from +6 in SO_4^{2-} to -2 in sulfides. The original pool of sulfur on Earth was held in igneous rocks, largely as pyrite (FeS_2). Degassing of the mantle and, later, weathering of the crust under an atmosphere containing O_2 transferred a large amount of S to the oceans, where it is now found as SO_4^{2-} (Table 2.3). When SO_4^{2-} is assimilated by organisms, it is reduced and converted into organic sulfur, which is an essential component of protein. However, the live biosphere contains relatively little sulfur. Today, the major global pools of S are found in biogenic pyrite, seawater, and evaporites derived from ocean water (Table 13.1).

Like sulfur, the majority of the Earth's mercury (Hg) is found in the crust, and it is released to the atmosphere and oceans by volcanic eruptions, rock weathering, and human activities. Human and microbial activities yield a global biogeochemical cycle for this element, which has long been recognized as toxic to life.

As in the case of nitrogen, microbial transformations between valence states drive the global S and Hg cycles. Under anoxic conditions, SO_4 is a substrate for sulfate reduction, which may lead to the release of reduced gases to the atmosphere and to the deposition of biogenic pyrite in sediments (Chapters 7 and 9). Anoxic environments can also support sulfur-based photosynthesis, which is likely to have been one of the first forms of

TABLE 13.1 Active Reservoirs of Sulfur near the Surface of the Earth

Reservoir	10^{18} g S
Atmosphere	0.0000028
Seawater	1280
Sedimentary rocks	
Evaporites	2470
Shales	4970
Land plants	0.0085
Soil organic matter	0.0155
Total	8720

Sources: From Holser et al. (1989) and Dobrovolsky (1994).

photosynthesis on Earth (Eq. 2.12). In the presence of oxygen, reduced sulfur compounds are oxidized by microbes. In some cases, the oxidation of S is coupled to the reduction of CO₂ in the reactions of S-based chemosynthesis (Eq. 4.6).

Mercury is transformed among valence states that include dissolved ions (Hg²⁺), elemental mercury (Hg⁰), and an especially toxic form known as methyl-mercury (CH₃Hg). Sulfate-reducing bacteria are implicated in the production of methyl-mercury in sediments, so the global cycles of S and Hg are linked by metabolism.

Understanding the biogeochemistry of S and Hg has enormous economic significance. Many metals are mined from sulfide minerals in hydrothermal ore deposits (Meyer 1985). Microbial reactions involving sulfur bacteria are used to concentrate metals from water (e.g., Zn, Labrenz et al. 2000; Cu, Sillitoe et al. 1996; and Au, Lengke and Southam 2006), and are used to remove metals from relatively low-grade ore (Lundgren and Silver 1980). Sulfur is an important constituent of both coal and oil. The organic S in coal is oxidized to sulfuric acid when coal is exposed to air. SO₂ is emitted to the atmosphere when coal and oil are burned.

A large amount of SO₂ is also emitted during the smelting of copper ores (Cullis and Hirschler 1980, Oppenheimer et al. 1985). An understanding of the relative importance of natural sulfur compounds in the atmosphere compared to anthropogenic SO₂ is essential to evaluate the causes of acid rain and the impact of acid rain on natural ecosystems. Similarly, understanding the natural and anthropogenic sources of mercury in the atmosphere allows rational policy decisions regarding the regulation of mercury emissions from power plants and other sources.

In this chapter, we compare the global cycles of S and Hg, since both are characterized by microbial reduction reactions that produce volatile forms. Assembling quantitative global cycles for these elements allows us to put the human emissions of S and Hg into a larger context. As we did for carbon (Chapter 11), nitrogen, and phosphorus (Chapter 12), we will attempt to establish a budget for S and Hg on land and in the atmosphere. Then we will couple these to marine budgets (Figure 9.29) to form an overall picture of the global cycles. The biogeochemical cycle of S has varied through Earth's history as a result of the appearance of new metabolic pathways and changes in their importance. We will review the history of the S cycle as it is told by sedimentary rocks.

THE GLOBAL SULFUR CYCLE

No sulfur gas is a long-lived or major constituent in the atmosphere. Thus, all attempts to model the global S cycle must explain the fate of the large annual input of sulfur compounds to the atmosphere. The short mean residence time for atmospheric sulfur compounds, as a result of their oxidation to SO_4 , allows us to express all the fluxes in the global budget in units of 10^{12} g of S, regardless of the original form of emission. Despite the small atmospheric content of S compounds (totaling $\sim 4 \times 10^{12}$ g S at any moment; Rodhe 1999), the annual flux of S compounds through the atmosphere (about 300×10^{12} g S/yr) rivals the movements of N in the global nitrogen cycle (compare Figure 13.1 to Figure 12.2).

In 1960, Eriksson examined the potential origins of SO_4 in Swedish rainfall and hence, indirectly, sources of SO_4 in the atmosphere. He reasoned that if all the Cl^- in rainfall is

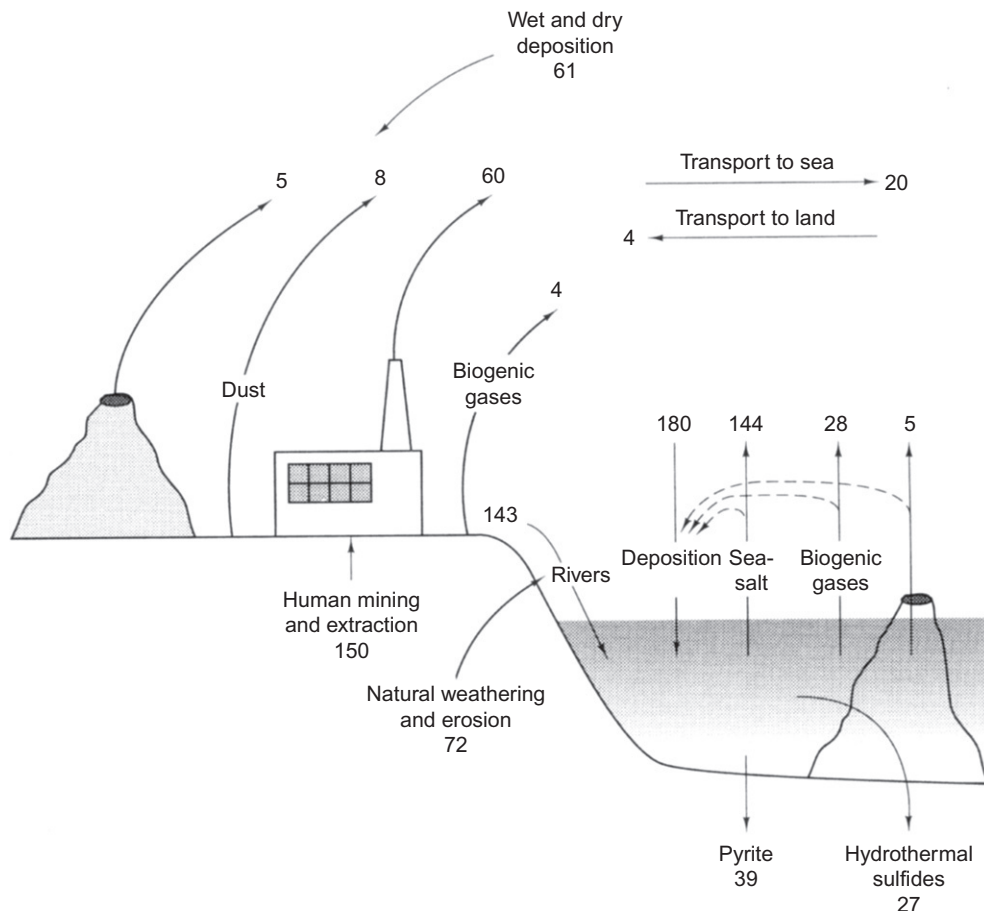


FIGURE 13.1 The global S cycle with annual flux shown in units of 10^{12} g S/yr. The derivation of most values is described in the text, with the marine values taken from Figure 9.22. The net flux from land to sea is extrapolated from Whelpdale and Galloway (1994).

derived from the ocean, then seaspray should also carry SO_4^{2-} roughly in proportion to the ratio of SO_4^{2-} to Cl^- in seawater. His calculation suggested that about 4×10^{12} g S/yr deposited on land must be derived from the sea. At about the same time, however, Junge (1960) was evaluating the SO_4 content of rainfall, and he estimated that about 73×10^{12} g S/yr was deposited on land globally. Clearly, there were other sources of SO_4 in the atmosphere and in rainfall. Junge's maps showed that SO_4 was abundant in the rainfall of industrial regions and in areas downwind of deserts (Figure 3.14a). Desert soils are a source of gypsum ($\text{CaSO}_4 \cdot 2\text{H}_2\text{O}$) in atmospheric dust (Reheis and Kihl 1995), and the burning of fossil fuels in industrial regions contributes SO_2 to air pollution (Langner et al. 1992, Spiro et al. 1992). By the mid 1970s, "acid rain" was clearly linked to coal-fired power plants, which release SO_2 (Likens and Bormann 1974). In the intervening years, new sources of S in the atmosphere have been recognized, and global flux estimates have been revised repeatedly. Our understanding of the global S cycle is much improved, but most of the estimates illustrated in Figure 13.1 remain subject to considerable uncertainty.

Episodic events, including volcanic eruptions and dust storms, contribute to the global biogeochemical cycle of S. Sulfur emissions from volcanoes are especially difficult and dangerous to measure. SO_2 dominates the volcanic release, but significant H_2S is reported in some eruptions (Aiuppa et al. 2005, Clarisse et al. 2011); both are oxidized to SO_4 in the atmosphere (compare to Eqs. 3.27–3.28). Legrand and Delmas (1987) used the deposition of SO_4 in the Antarctic ice pack to estimate the contribution of volcanoes to the global S cycle during the last 220 years. The Tambora eruption of 1815 was the largest, releasing 50×10^{12} g S to the atmosphere. Typically, major eruptions, such as that of Mt. Pinatubo (15 June 1991), release 5 to 10×10^{12} g S each (Bluth et al. 1993).

Following a major volcanic eruption, the Earth's climate is cooled for several years, as a result of SO_4 aerosols in the stratosphere (Briffa et al. 1998, McCormick et al. 1995, Rampino et al. 1988). When the volcanic emissions are averaged over many years, the annual global flux is about 7.5 to 10.5×10^{12} g S/yr (Halmer et al. 2002). About 70% of the sulfur gases leak passively from volcanoes and the remainder is derived from periodic, explosive events (Bluth et al. 1993, Allard et al. 1994). Huge eruptions in the Late Cretaceous (66 mya) may have released more than 1000 Tg S to the atmosphere (Self et al. 2008).

The movement of S in soil dust is also episodic and poorly understood. Many of the large particles are deposited locally, while smaller particles may undergo long-range transport in the atmosphere (Chapter 3). Savoie et al. (1987) found that dust from the deserts of the Middle East contributes SO_4 to the waters of the northwest Indian Ocean. Ivanov (1983) suggests a global flux of 8×10^{12} g S/yr owing to dust transport in the troposphere—about 10% of the fossil fuel release.

The total flux of biogenic sulfur gases from land is likely $<4 \times 10^{15}$ g S/yr (Watts 2000). The dominant sulfur gas emitted from freshwater wetlands and anoxic soils is H_2S , with dimethylsulfide and carbonyl sulfide (COS) playing lesser roles (Chapter 7). Emissions from plants are poorly understood and deserving of further study (Chapter 6). Forest fires emit an additional 2×10^{12} g S/yr (Andreae and Merlet 2001, Kaiser et al. 2012).

It seems certain that direct emissions from human industrial activities are the largest sources of S gases in the atmosphere. Ice cores from Greenland show a large increase in the deposition of SO_4 from the atmosphere at the beginning of the Industrial Revolution (Herron et al. 1977; Mayewski et al. 1986, 1990; Fischer et al. 1998). In Europe and the

United States, these emissions have been sharply curtailed by the control of air pollution in recent years (Likens et al. 2005, Stern 2006, Velders et al. 2011), and the SO_4 content in rainfall has fallen in parallel (Figure 13.2). Estimates of the recent global flux range from 50 to 70×10^{12} g S/yr (Smith et al. 2001a, Faloona 2009, Lee et al. 2011).

Owing to the reactivity of S gases in the atmosphere, most of the anthropogenic emission of SO_2 is deposited locally in precipitation and dryfall. Total deposition of S on land may be as high as 120×10^{12} g S/yr (Andreae and Jaeschke 1992), but a value of $\sim 60 \times 10^{12}$ g S/yr balances the global S cycle shown in Figure 13.1. Deposition in dryfall and the direct absorption of SO_2 are poorly understood, so this global estimate is subject to revision. The estimate of atmospheric deposition on land accounts for a large fraction of the total emissions from land. The remainder undergoes long-distance transport in the atmosphere and accounts for a net transfer of S from land to sea (Whelpdale and Galloway 1994).

A small fraction of the natural river load of SO_4 is derived from rainfall, which includes cyclic salts that are carried through the atmosphere from the ocean (4×10^{12} g S/yr in Figure 13.1). Weathering of pyrite and gypsum also contributes to the SO_4 content of river water (Table 4.9). The remainder of the global flux of S in rivers is derived from human activities. Berner (1971) suggested that at least 28% of the SO_4 content of modern rivers is derived from air pollution, mining, erosion, and other human activities. Meybeck (1979) estimates that the current river transport of about 143×10^{12} g S/yr is roughly double that of preindustrial conditions.

The marine portion of the global S cycle is largely taken from Figure 9.29. The ocean is a large source of seasalt aerosols that contain SO_4 , but most of these are redeposited in the ocean in precipitation and dryfall. Dimethylsulfide— $(\text{CH}_3)_2\text{S}$, or DMS—is the major biogenic gas

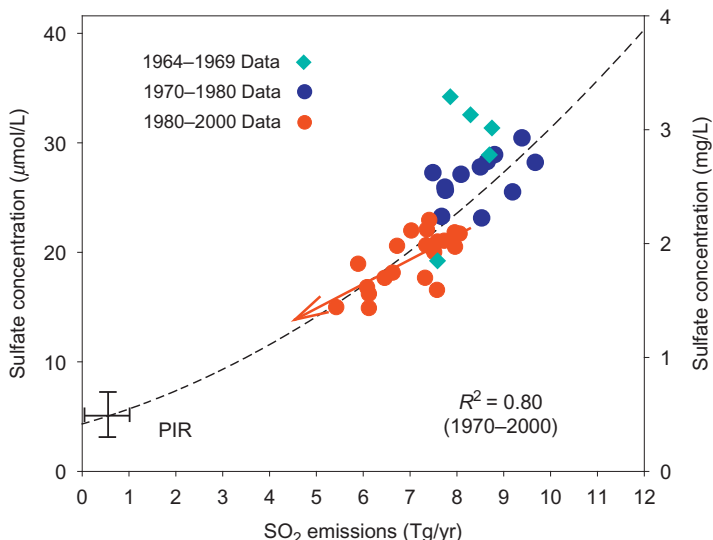


FIGURE 13.2 Sulfate concentration in wetfall precipitation at New Hampshire's Hubbard Brook Experimental Forest, as a function of SO_2 emissions in the estimated 24-hr source area. This shows the decline in both parameters as a result of the implementation of the Clean Air Act. (PRI shows the levels of the pre-industrial revolution.) Source: From Likens et al. 2005. Used with permission of RSC Publishing, copyright Royal Society of Chemistry.

emitted from the sea, with a global annual flux of 10 to 30×10^{12} g S/yr (Faloona 2009) and a recent best estimate of 28 Tg S/yr (Lana et al. 2011; [Chapter 9](#)). Thus, DMS is the largest natural source of sulfur gases in the atmosphere. The mean residence time of DMS in the atmosphere is < 2 days ([Table 3.5](#)), as a result of its oxidation to SO₂. Much of the SO₂ is further oxidized to SO₄ (Faloona et al. 2009). Thus, most of the sulfur from DMS is also redeposited in the oceans.

In addition to helping balance the marine sulfur budget, dimethylsulfide attains global significance for its potential effects on climate (Shaw 1983). Charlson et al. (1987) postulated that the oxidation of DMS to sulfate aerosols would increase the scattering of solar radiation and the abundance of cloud condensation nuclei in the atmosphere, leading to greater cloudiness (Bates et al. 1987). Clouds over the sea reflect incoming sunlight, leading to global cooling ([Chapter 3](#)). SO₄ aerosols in the marine atmosphere, or deposited from it, that are not derived from seawater are known as non-seasalt sulfate (nss-sulfate), and are indicative of emissions of DMS, volcanoes, and other biogenic gases (Xie et al. 2002). A significant portion of the SO₄ in the Antarctic icepack and exposed soils is nss-sulfate, potentially from DMS (Legrand et al. 1991, Bao et al. 2000).

The hypothesis that DMS might provide a biotic regulation on global temperature is intriguing, for it may be responsible for the moderation of global climate throughout geologic time. If higher marine NPP is associated with warmer sea surface temperatures, then a greater flux of DMS would have the potential to act as a negative feedback on global warming through the greenhouse effect. Given the strong arguments pointing to global warming by increased atmospheric CO₂, the potential negative feedbacks of DMS are the subject of intense scientific scrutiny and debate. For instance, Quinn and Bates (2011) question the role of SO₄²⁻ aerosols derived from DMS versus the production of a variety of other aerosols in the marine atmosphere.

The production of DMS is often related to the growth of certain marine phytoplankton (Andreae et al. 1994a, Steinke et al. 2002). DMS flux is directly correlated to solar irradiance (Vallina and Simo 2007, Gali et al. 2011). The flux of DMS from the sea is greater in summer than in winter, as a result of greater sea surface temperature (Prospero et al. 1991, Tarrasón et al. 1995). The concentration of DMS in seawater is well correlated to that in the air over the North Pacific Ocean (Watanabe et al. 1995).

Cloud condensation nuclei also appear to be well correlated to the atmospheric burden of DMS in nonpolluted areas (Ayers and Gras 1991, Putaud et al. 1993, Andreae et al. 1995). The ice-core record of methanesulphonate (MSA)—a DMS degradation product—suggests higher concentrations during the last glacial epoch than today (Legrand et al. 1991, but see Castebrunet et al. 2006). Certainly the ocean's temperature was lower during the last glacial, but if, for other reasons (e.g., a greater deposition of iron-rich dust), marine NPP productivity was higher during the last glacial, an increased flux of DMS may have reinforced the global cooling of Earth's climate. Indeed, Turner et al. (1996) report more than a threefold increase in DMS flux to the atmosphere during an iron-enrichment experiment in the Pacific Ocean. If natural emissions of DMS increase in the future, it is possible that they will act to dampen the greenhouse effect during the next century.

The potential for atmospheric SO₄ aerosols to cool Earth's climate is clearly seen in observations of global temperature after major explosive volcanic events which inject S gases into the stratosphere. Schwartz (1988) argued that anthropogenic emissions of SO₂ should have the same effect on global climate as natural emissions of DMS, because SO₂ is also oxidized to produce condensation nuclei in the atmosphere. Most of the anthropogenic SO₂ emissions derive

from land. Only about 4×10^{12} g S are emitted as SO₂ by international shipping (Corbett et al. 1999), and a very small additional amount by aircraft (Kjellstrom et al. 1999).

Using a general circulation model for global climate, Wigley (1989) suggested that climatic cooling by SO₂, largely from coal-fired power plants, may have offset some of the temperature change expected from the greenhouse effect, especially before the institution of air pollution controls in the United States and Europe. The Earth's albedo has apparently increased slightly in recent years, presumably due to particulate air pollutants (Pallé et al. 2009, Wang et al. 2009). Greater albedo reduces the radiation reaching the Earth's surface (i.e., global dimming). Reductions in man-made sulfur emissions might exacerbate global warming because the cooling effect of sulfur aerosols will be removed (Andreae et al. 2005). Because SO₂ has a short atmospheric lifetime (Chapter 3), its effect is regional and centered on areas of industry (Kiehl and Briegleb 1993, Falkowski et al. 1992, Langner et al. 1992). Some workers have even suggested injecting SO₄-forming aerosols into the stratosphere as a means of reducing Earth's temperature—a form of geo-engineering in response to the greenhouse warming of our planet (Crutzen 2006). This suggestion is not without controversy, given the potential for inadvertent impacts on the biosphere (Robock et al. 2009).

Temporal Perspectives on the Global Sulfur Cycle

During the accretion of the primordial Earth, sulfur was among the gases that were released by degassing of the Earth's mantle to form the secondary atmosphere (Chapter 2). Even today, volcanic emissions contain appreciable concentrations of SO₂ and H₂S (Table 2.2). When the oceans condensed on Earth, the atmosphere was essentially swept clear of S gases, owing to their high solubility in water (Eq. 2.6). On Venus, where there is no ocean, crustal degassing has resulted in a large concentration of SO₂ in the atmosphere (Oyama et al. 1979). The dominant form of S in the earliest seawater is likely to have been SO₄²⁻; high concentrations of Fe²⁺ in the primitive ocean would have precipitated any sulfides, which are insoluble under anoxic conditions (Walker and Brimblecombe 1985). Nevertheless, the SO₄ content of the earliest oceans was low (Habicht et al. 2002) and increased in concert with the rise of O₂ in Earth's atmosphere (Canfield et al. 2000). The total inventory of S compounds on the surface of the Earth (nearly 10^{22} g S) represents the total crustal outgassing of S through geologic time (Table 2.3).

The ratio of ³²S to ³⁴S in the total S inventory on Earth is thought to be similar to the ratio of 22.22 measured in the Canyon Diablo Troilite (CDT), a meteorite collected in Arizona. The sulfur isotope ratio in this rock is accepted as an international standard and assigned a value of 0.00. In other samples, deviations from this ratio are expressed as $\delta^{34}\text{S}$, with the units of parts per thousand parts (‰)—a convention that we also used for the isotopes of carbon (Chapter 5) and nitrogen (Chapter 6). Presumably the $\delta^{34}\text{S}$ isotope ratio in the earliest oceans was 0.00, because there is no reason to expect any discrimination between the isotopes of S during crustal degassing. When evaporite minerals precipitate from seawater, there is little differentiation among the isotopes of sulfur, so geologic deposits of gypsum (CaSO₄·2H₂O) and barite (BaSO₄) carry a record of the isotopic composition of S in seawater. In the earliest sedimentary rocks, dating to 3.8 bya, $\delta^{34}\text{S}$ is close to 0.00 (Schidlowski et al. 1983).

Dissimilatory sulfate reduction by bacteria strongly differentiates among the isotopes of sulfur, as a result of a more rapid enzymatic reaction with ³²SO₄. By itself, sulfate metabolism results in an isotopic depletion of -18‰ $\delta^{34}\text{S}$ in H₂S and sedimentary sulfides relative to the ratio in the

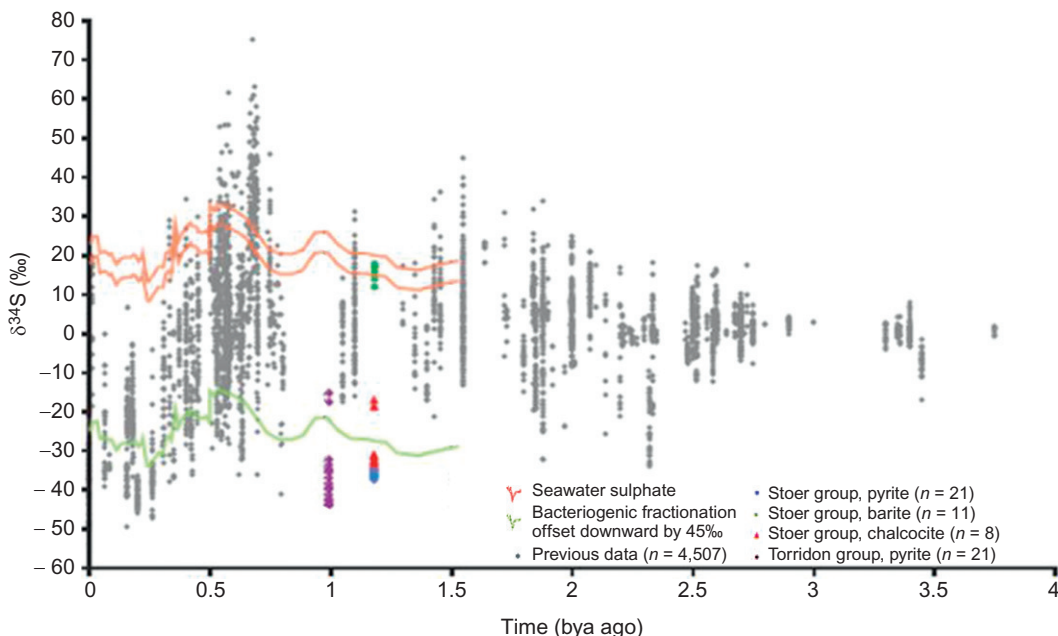


FIGURE 13.3 $\delta^{34}\text{S}$ in sedimentary pyrites through geologic time. Source: Modified from Parnell et al. (2010).

source reservoir (Canfield and Teske 1996). Stronger fractionations, sometimes as much as $-66\text{\textperthousand}$, are also reported (Sim et al. 2011). Strongly depleted sedimentary sulfides can result from repeated cycles of oxidation and reduction (Canfield and Teske 1996) and the reduction of thiosulfate ($\text{S}_2\text{O}_3^{2-}$) and sulfite ($\text{S}_2\text{O}_3^{2-}$) in sediments (Canfield and Thamdrup 1994, Habicht et al. 1998). The evolution of sulfate reduction dates to 2.4 to 2.7 bya, based on the first occurrence of sedimentary rocks with depletion of ^{34}S (Cameron 1982, Schidlowski et al. 1983, Habicht and Canfield 1996; Figure 13.3).¹ This also marks the time of the first substantial SO_4 concentrations in the primitive oceans. Today, the average $\delta^{34}\text{S}$ in sedimentary sulfides in all of the Earth's crust is about -10 to $-12\text{\textperthousand}$ (Holser and Kaplan 1966, Migdisov et al. 1983).

Figure 13.4 shows a three-box model for the S cycle, in which marine SO_4 and sedimentary sulfides are connected through microbial oxidation and reduction reactions, which discriminate between the sulfur isotopes (compare to Garrels and Lerman 1981). During periods of Earth's history when large amounts of sedimentary pyrite were formed as a result of sulfate reduction, seawater SO_4 became enriched in residual $^{34}\text{SO}_4$. Meanwhile, deposition or dissolution of evaporate deposits has no effect on the isotopic composition of seawater, but can strongly affect the concentration of SO_4 in seawater and thus the rate of sulfate-reduction and pyrite deposition (Wortmann and Paytan 2012).

Currently, about 50% of the pool of S near the surface of the Earth is found in reduced form (Li 1972, Holser et al. 1989), and the $\delta^{34}\text{S}$ of seawater is $+21\text{\textperthousand}$ (Kaplan 1975, Rees et al. 1978). Because there is little differentiation among isotopes of S during the precipitation of evaporites, the sedimentary record of evaporites indicates changes in the $\delta^{34}\text{S}$ of seawater over

¹ Scattered evidence is found for S-reduction as early as 3.4 bya (Ohmoto et al. 1993, Shen et al. 2001).

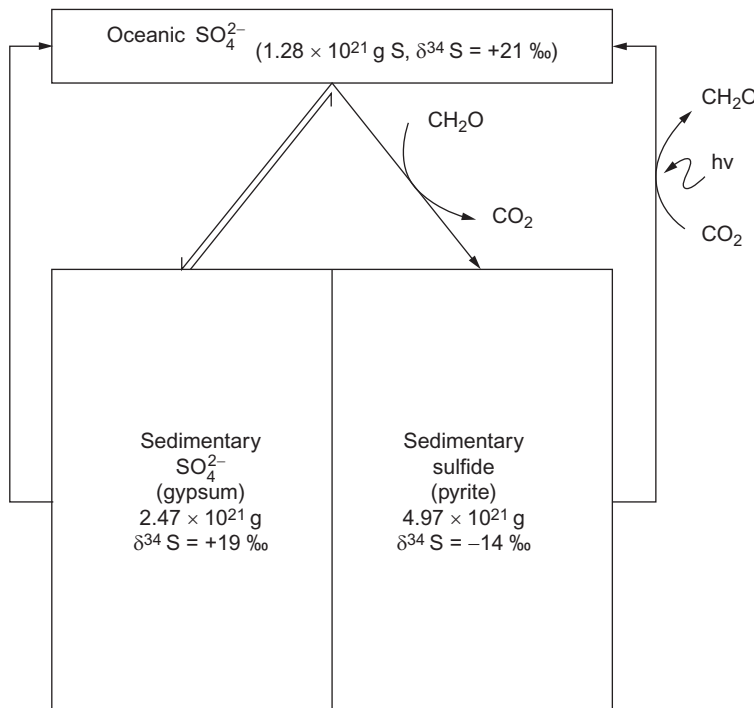


FIGURE 13.4 A model for the global sulfur cycle, showing the linkage and partitioning of S between oxidized and reduced pools near the surface of the Earth. Transfers of S from seawater to pyrite involve a major fractionation between ^{34}S and ^{32}S isotopes, whereas exchange between seawater SO_4 and sedimentary SO_4 (largely gypsum) involves only minor fractionation. The sum of all pools, nearly 10^{22} g S, represents the total outgassing of S from the mantle (compare to Table 2.3). About 15% now resides in the ocean. Estimates of the pool of S in sedimentary sulfides show a wide range of values; the value here, from Holser et al. (1989), is close to that estimated from the pool of sedimentary organic carbon (1.56×10^{22} g; Des Marais et al. 1992) divided by the mean C/S ratio in marine sediments (2.8; Raiswell and Berner 1986). Isotope ratios in seawater and gypsum are taken from Holser et al. (1989). The isotope rate of S in sedimentary sulfides is derived by mass balance to yield $\delta^{34}\text{S}$ of +4.2 in the global inventory.

geologic time. Changes in the isotopic composition of seawater indicate changes in the relative size of the reservoir of sedimentary pyrite, which occur as a result of changes in the net global balance between sulfate reduction and the oxidation of sedimentary sulfides ($\sim 100 \times 10^{12}$ g S/yr). By contrast, the annual uptake of S by marine phytoplankton and release through their decomposition ($\sim 1390 \times 10^{12}$ g S/yr; Dobrovolsky 1994, p. 183) have little effect on the isotopic composition of the major reservoirs of the global S cycle.

During the last 600,000,000 years, seawater SO_4 has varied between +10 and +30‰ in $\delta^{34}\text{S}$ (Figure 13.5), with an average value close to that of today. Seawater sulfate shows a marked positive excursion (+32‰) in $\delta^{34}\text{S}$ during the Cambrian (550 mya), when the deposition of pyrite must have been greatly in excess of the oxidation of sulfide minerals exposed on land. Seawater sulfate was less concentrated in ^{34}S , that is, $\delta^{34}\text{S}$ of +10‰, during the Carboniferous and Permian, when a large proportion of the Earth's net primary production occurred in freshwater swamps, where SO_4 , sulfate reduction, and pyrite deposition are less important

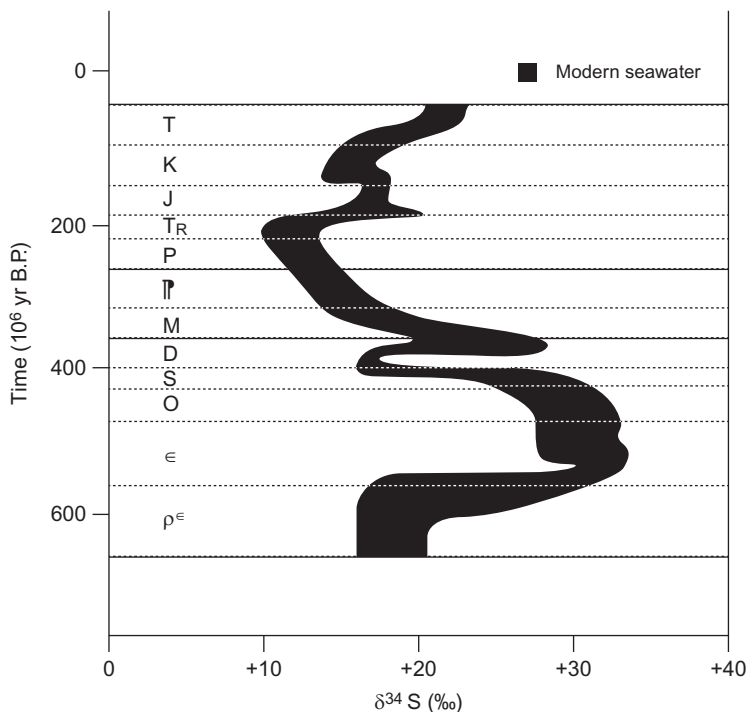


FIGURE 13.5 Variations in the isotopic composition of seawater SO_4 through geologic time. *Source: From Kaplan (1975). Used with permission from the Royal Society of London.*

(Berner 1984). Presumably the concentration of SO_4 in seawater was also greater during that interval, because the global rate of pyrite formation was depressed. The record of $\delta^{34}\text{S}$ in marine barite fluctuates in an inverse correlation with records of marine productivity during the past 130 million years (Paytan et al. 2004).

Although the sulfur cycle has shown shifts between net sulfur oxidation and net sulfur reduction in the geologic past, the current human impact is probably unprecedented in the geologic record. As we found for the carbon cycle, the present-day cycle of S is not in steady state. Human activities have added a large flux of gaseous sulfur to the atmosphere, some of which is transported globally. Humans are mining coal and extracting petroleum from the Earth's crust at a rate that mobilizes $150 \times 10^{12} \text{ g S/yr}$, more than double the rate of 100 years ago (Brimblecombe et al. 1989). The net effect of these processes is to increase the pool of oxidized sulfur (SO_4) in the global cycle, at the expense of the storage of reduced sulfur in the Earth's crust. The current estimates of inputs to the ocean are slightly in excess of the estimate of total sinks, implying that the oceans are increasing in SO_4 by over 10^{13} g S/yr . Such an increase will be difficult to document because the content in the oceans is $1.28 \times 10^{21} \text{ g S}$. As calculated in Chapter 9, the mean residence time for SO_4 in seawater is about 10,000,000 years with respect to the current inputs from rivers.

Various workers have attempted to use measurements of $\delta^{34}\text{S}$ to deduce the origin of the SO_4 in rainfall and the extent of human impact on the movement of S in the atmosphere (Grey and Jensen 1972, Nriagu et al. 1991, Mast et al. 2001, Puig et al. 2008). Unfortunately, the

potential sources of SO_4 show a wide range of values for $\delta^{34}\text{S}$, making the identification of specific sources difficult (Nielsen 1974). For example, the sulfur in coal may be depleted in $\delta^{34}\text{S}$ if it is found as pyrite or enriched in $\delta^{34}\text{S}$ if it is derived from the sulfur that was originally assimilated by the plants forming coal (Hackley and Anderson 1986). Thus, coals show a wide range in $\delta^{34}\text{S}$. Similarly, petroleum shows a range of -10.0 to $+25\text{\textperthousand}$ in ^{34}S (Krouse and McCready 1979). Desert dusts containing SO_4 show a wide range in $\delta^{34}\text{S}$, averaging $+5.8\text{\textperthousand}$ (Bao and Reheis 2003). In the eastern United States, $\delta^{34}\text{S}$ of rainfall varies seasonally between $+6.4\text{\textperthousand}$ in winter and $+2.9\text{\textperthousand}$ in summer, consistent with any of these sources or a combination of them (Nriagu and Coker 1978). The lower values of summer are thought to reflect the influence of biogenic sulfur derived from sulfate reduction in wetlands (Nriagu et al. 1987).

When SO_2 is emitted as an air pollutant, it forms sulfuric acid through heterogeneous reactions with water in the atmosphere (Eqs. 3.27–3.30). As a strong acid that is completely dissociated in water, H_2SO_4 suppresses the disassociation of natural, weak acids in rainfall. For example, in the absence of strong acids, the dissolution of CO_2 in water will form a weak solution of carbonic acid, H_2CO_3 , and rainfall pH will be about 5.6:



In the presence of strong acids that lower the pH below 4.3, this reaction moves to the left, and carbonic acid makes no contribution to free acidity. In many industrialized areas, free acidity in precipitation is almost wholly determined by the concentration of the strong acid anions, SO_4^{2-} and NO_3^- (Table 13.2). Rock weathering that was primarily driven by carbonation weathering in the preindustrial age is now driven by anthropogenic H^+ (Johnson et al. 1972).

TABLE 13.2 Sources of Acidity in Acid Rainfall Collected in Ithaca, New York, on July 11, 1975
(ambient pH 3.84)

Component	Concentration in precipitation (mg/liter)	Contribution to	
		Free acidity at pH 3.84 ($\mu\text{eq/liter}$)	Total acidity in a titration to pH 9.0 ($\mu\text{eq/liter}$)
H_2CO_3	0.62	0	20
Clay	5	0	5
NH_4^+	0.53	0	29
Dissolved Al	0.050	0	5
Dissolved Fe	0.040	0	2
Dissolved Mn	0.005	0	0.1
Total organic acids	0.43	2	5.7
HNO_3	2.80	40	40
H_2SO_4	5.60	102	103
Total		144	210

Source: From Galloway et al. (1976). Copyright 1976 by the American Association for the Advancement of Science. Used with permission.

It is interesting to estimate the global sources of acidity in the atmosphere. In this analysis, we are only interested in reactions that are net sources of H^+ , so we can ignore the movements of soil dusts and seaspray because the strong-acid anions they contain, NO_3^- and SO_4^{2-} , are largely balanced by cations (especially Ca and Na) that are emitted at the same time. If the pH of all rainfall on Earth was 5.6 as a result of an equilibrium with atmospheric CO_2 , the total deposition of H^+ ions would be 1.24×10^{12} moles/year. The production of NO by lightning produces additional acidity because NO dissolves in rainwater, forming HNO_3 .

Globally, N fixation by lightning contributes 0.36×10^{12} moles of H^+/yr , and other natural sources of NO_x (soils and forest fires) contribute 1.57×10^{12} moles of H^+/yr . In the years following massive eruptions, SO_2 from volcanoes is distributed globally and dominates the atmospheric deposition of S (Mayewski et al. 1990, Langway et al. 1995). On average, however, volcanic emanations of SO_2 contribute $\sim 0.56 \times 10^{12}$ moles H^+/yr , and the oxidation of biogenic S gases produces 1.76×10^{12} moles H^+/yr . Thus, the total, natural production of H^+ in the atmosphere is normally about 4.25×10^{12} moles/ yr . In contrast, the anthropogenic production of NO_x and SO_2 results in about 5.53×10^{12} moles of H^+/year —more than all natural sources of acidity combined.

The only net source of alkalinity in the atmosphere comes from the reaction of NH_3 with the strong acids H_2SO_4 and HNO_3 to form aerosols, $(\text{NH}_4)_2\text{SO}_4$ and NH_4NO_3 (Eq. 3.5). However, the “natural” global emission of NH_3 , about 19×10^{12} g N/ yr (Table 12.2), reduces the “natural” production of H^+ by only about 1.37×10^{12} moles/ year , or 32% (compare to Savoie et al. 1993). Thus, even though the current acidity of the atmosphere is much higher as a result of human activities, the atmosphere has always acted as an acidic medium with respect to the Earth’s crust throughout geologic time. Anthropogenic emissions of NH_3 neutralize 2.44×10^{12} moles H^+/yr , or 44% of the anthropogenic emissions of the acid-forming gases, NO_x and SO_2 .

The Atmospheric Budget of Carbonyl Sulfide

Showing an average concentration of about 500 parts per trillion, carbonyl sulfide (COS ; alternatively OCS) is the most abundant sulfur gas in the atmosphere (Table 3.1). The pool in the atmosphere contains about 2.8×10^{12} g S (Chin and Davis 1995). Based on the global budget shown in Table 13.3, the mean residence time for COS in the atmosphere is ~ 5 years. COS shows seasonal fluctuations in the atmosphere, parallel to CO_2 and likely to reflect plant activity (Montzka et al. 2004, 2007; Campbell et al. 2008; Geng and Mu 2006).

The global budget for COS in the atmosphere has been revised repeatedly during the last few decades (compare Khalil and Rasmussen 1984, Servant 1989, Chin and Davis 1995, Watts 2000, Kettle et al. 2002), and the current budget of COS is slightly imbalanced—showing an excess of sources over sinks. Several components of the budget, including net ocean uptake, are poorly constrained. The concentration of COS in the atmosphere has increased during the Industrial Revolution (Aydin et al. 2002, Montzka et al. 2004), but it declined slightly during the past couple of decades (Sturges et al. 2001, Rinsland et al. 2002).

The major source of COS in the atmosphere stems from the oxidation of carbon disulfide (CS_2) emitted from anoxic soils and industrial sources. The oceans are an indirect source of

TABLE 13.3 Global Budget for Carbonyl Sulfide in the Atmosphere

Sources	COS (10^{12} g S/yr)
Oceans	0.04 ^a
Anoxic soils	0.03
Biomass burning	0.04 ^b
Fossil fuels	0.06
Volcanoes	0.02
Oxidation of CS ₂	0.25 ^c
Oxidation of DMS	0.16
Total sources	0.60
<hr/>	
Sinks	
Vegetation uptake	0.24
Soil uptake (oxic)	0.13
Oxidation by OH	0.09
Stratospheric photolysis	0.02
Total sinks	0.48

^a Net.^b Compare, 0.14 Tg S/yr; Andreae and Merlet (2001).^c 44% from anthropogenic sources.

Sources: From Kettle et al. (2002), except volcanic flux (Chin and Davis 1993).

COS, stemming from the oxidation of DMS. A small amount of COS is produced by the photochemical destruction of dissolved organic matter in seawater (Ferek and Andreae 1984). In the global budget (Table 13.3), the small direct source of COS from the oceans is a net value, recognizing that COS is also taken up by seawater (Weiss et al. 1995). Other sources of COS include biomass burning (Nguyen et al. 1995, Andreae and Merlet 2001) and direct industrial emissions. Wetland soils are a small source, but the global emission of COS from salt marshes is limited by the small extent of salt marsh vegetation (Aneja et al. 1979, Steudler and Peterson 1985, Carroll et al. 1986).

Some COS is oxidized in the troposphere via OH radicals, but the major tropospheric sink for COS, first reported by Goldan et al. (1988), appears to be uptake by vegetation and upland, oxic soils (Steinbacher et al. 2004, Kuhn et al. 1999, Simmons et al. 1999). Indeed, several workers have suggested that measurements of the uptake of COS through plant stomata may be useful as a measure of *gross primary production* (Stimler et al. 2010, Blonquist et al. 2011, Wohlfahrt et al. 2012). Kesselmeier and Merk (1993) found that a variety of crop plants take up COS whenever the ambient concentration is greater than 150 ppt. Uptake by vegetation is now believed to account for half of the total annual destruction of COS globally (Table 13.3).

A small amount of COS is mixed into the stratosphere, where it is destroyed by a photochemical reaction involving the OH radicals, producing SO₄ (Chapter 3). In fact, aside from the periodic eruptions of large volcanoes, COS appears to be the main source of SO₄ aerosols in the stratosphere (Hofmann and Rosen 1983, Servant 1986). There is some evidence that these aerosols have increased in recent years (Hofmann 1990). In the absence of trend toward increasing COS, some workers have suggested that SO₂ from high-altitude aircraft may be responsible (Hofmann 1991). These aerosols affect the amount of solar radiation entering the troposphere, and they are an important component of the radiation budget of the Earth (Turco et al. 1980). Through direct and indirect (CS₂) sources, humans appear to make large contributions to the budget of COS (Table 13.3), and any increase in COS-derived aerosols in the stratosphere has potential consequences for predictive models of future global warming (Hofmann and Rosen 1980). In return, global warming and an increasing flux of uvB radiation penetrating to the Earth's surface may enhance the production of COS in ocean waters (Najjar et al. 1995).

THE GLOBAL MERCURY CYCLE

Mercury is found as a trace metal in igneous rocks and is locally concentrated in economic deposits of a red mineral known as cinnabar (HgS) that is often associated with hydrothermally altered rock. Volcanoes are a large natural source of mercury emissions to Earth's atmosphere, in the form of elemental mercury, Hg⁰—a volatile metal (Siegel and Siegel 1984, Engle et al. 2006, Pyle and Mather 2003, Bagnato et al. 2011; Figure 13.6). Hg⁰ is oxidized

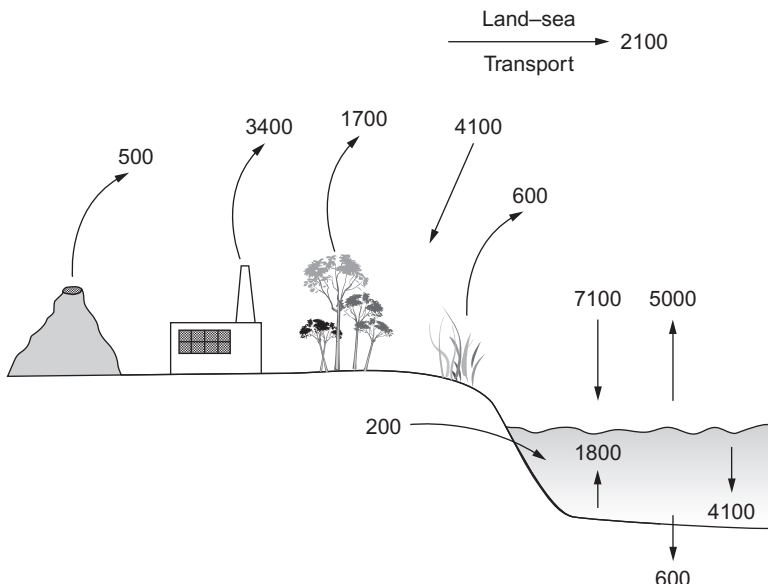


FIGURE 13.6 The global mercury cycle of the modern world. All values are 10^6 g Hg/yr. Source: From Selin (2009).

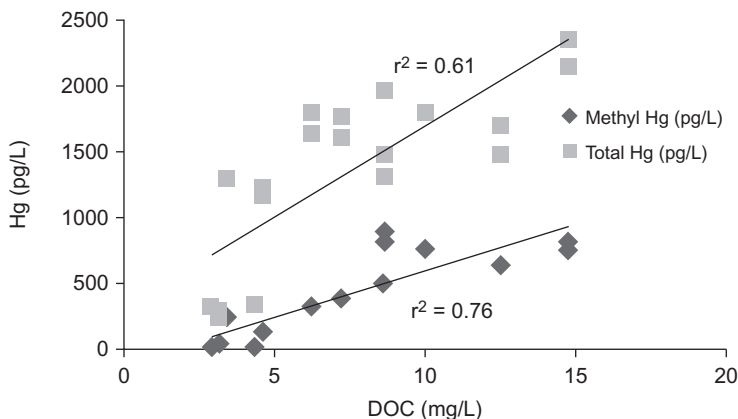


FIGURE 13.7 Concentration of total and methylmercury in stream waters draining into Lake Sunapee, New Hampshire as a function of the concentration of dissolved organic carbon. *Source: From Kathleen Weathers et al., unpublished.*

in the atmosphere to Hg^{2+} , which is the dominant form found in wet and dry deposition at the Earth's surface (Lin and Pehkonen 1999). The lifetime of Hg in the atmosphere ranges from about one year for Hg^0 to a few weeks for Hg^{2+} , so mercury shows regional patterns of deposition that reflect local emissions from natural sources and power plants (Engle et al. 2010, Prestbo and Gay 2009).

Rock weathering releases a small amount of mercury to runoff waters as Hg^{2+} (Figure 13.6). Humans have enhanced the flux of Hg from the Earth's crust by direct mining of mercury and others ores and by the combustion of coal (Pirrone et al. 2010, Gratz and Keeler 2011). As it circulates at the Earth's surface, mercury is rapidly converted among Hg^0 , Hg^{2+} , and particulate forms. When mercury is deposited in forests, some is reduced to Hg^0 and re-volatilized to the atmosphere (Graydon et al. 2012), while the remainder accumulates in soil organic matter (Demers et al. 2007, Gabriel et al. 2012) or binds to organic compounds that are transported in stream water (Dittman et al. 2010; Figure 13.7).

Similarly, some Hg^{2+} that is deposited in the oceans is photoreduced to elemental mercury that volatilizes from the ocean's surface, as a function of wind speed and Henry's Law for the dissolution of soluble gases in water (Andersson et al. 2008, Mason and Fitzgerald 1993, Kuss et al. 2011). Mercury tends to accumulate in polar ecosystems (Johnson et al. 2008b). Here the deposition of Hg is enhanced by a rapid oxidation to Hg^{2+} , probably mediated by atmospheric Br (Ariya et al. 2004, Jitaru et al. 2009).

Mercury has a long history of economic uses that led to the early human exploitation of ore deposits (Pacyna et al. 2006, Pirrone et al. 2010). Before its toxic properties were well known, mercury was widely used as a fungicide and as a preservative for leather, paint, and other products subject to microbial degradation.² Mercury has long been used to extract trace quantities of gold and other metals, and mining activities are often a source of mercury pollution

² See Act V, Scene 1 in Shakespeare's *Hamlet*, where the gravediggers comment that a hatmaker's corpse will decompose slowly, presumably because its content of mercury will impede microbial activity.

today (Pfeiffer et al. 1991, Artaxo et al. 2000). Mercury accumulates in organic sediments and coal, and is released to the atmosphere when these are burned (Billings and Matson 1972, Lee et al. 2006). Emissions of Hg rose to high values in the late 1800s, associated with the gold rush in the western United States, and again after World War II, associated with the proliferation of coal-fired power plants (Streets et al. 2011; compare Xu et al. 2011).

Lake sediments in New England and the Rocky Mountains show higher, recent levels of mercury accumulation than several centuries ago (Kamman and Engstrom 2002, Mast et al. 2010). Enhanced recent levels of mercury deposition are also recorded in peat bogs, where modern rates are elevated more than 15 times over those of the preindustrial period (Martinez-Cortizas et al. 1999, Roos-Barracough et al. 2002, Shotyk et al. 2003). Accumulations are often greater in colder periods, when low temperatures reduce the revolatilization of Hg from sediments (Martinez-Cortizas et al. 1999).

An especially toxic form of mercury, methylmercury (CH_3Hg^+ ,³) is produced by sulfate-reducing bacteria in anoxic sediments (Compeau and Bartha 1985; King et al. 2001; Gilmour et al. 1992, 2011; Schaefer and Morel 2009). The methylation process proceeds most rapidly with dissolved mercury (Hg^{2+}) and mercury associated with nanoparticles (Zhang et al. 2012b). Mercury accumulates in fishes as they age (Bache et al. 1971, Barber et al. 1972) and at progressively higher levels of food chains, so that large predatory fish often have the highest levels (Cabana and Rasmussen 1994). Higher concentrations of methylmercury are found in modern seabirds than in museum specimens of the same species collected a century ago (Monteiro and Furness 1997, Vo et al. 2011). Methylmercury is degraded by sunlight to Hg^0 , which is revolatilized from the surface of lakes and ocean waters (Mason and Fitzgerald 1993, Sellers et al. 1996, Black et al. 2012).

Methylmercury is found in fishes in nearly all waters of the United States (Scudder et al. 2009). When toxic levels of mercury were found in many freshwater and saltwater fishes in the 1970s, environmental regulations were implemented to reduce airborne emissions, especially from coal-fired power plants. Concentrations of mercury in the atmosphere now show a declining trend (Butler et al. 2008, Slemr et al. 2011), which is expected to yield a dramatic decline of mercury deposition from the atmosphere and declining levels in fish (Harris et al. 2007).

Enormous controversy has accompanied the establishment of policies to regulate mercury emissions to the atmosphere. Biogeochemists have helped to elucidate how much of the deposition in various areas is due to local, regional, or global sources (Sigler and Lee 2006, Selin et al. 2008, Weiss-Penzias et al. 2011, Gratz and Keeler 2011). Similarly, biogeochemistry shows how methylmercury forms during sulfate reduction in sediments and explains why the fish in some lakes have relatively low concentrations while those in nearby lakes, often those with organic sediments, may have higher concentrations (Chen et al. 2005, Ward et al. 2010). Sulfate-reducing bacteria and SO_4 -based acid rain are implicated in the methylation process (Gilmour and Henry 1991). The mercury content of river waters is controlled by chemical reactions in the water and by the types of environments that are a source of drainage (Burns et al. 2012). For Hg in the marine environment, we still have a poor understanding of the processes that produce methylmercury in seawater and contamination of marine fishes (Malcolm et al. 2010).

³ Often abbreviated MeHg.

SUMMARY

The major pool of S in the global cycle is found in the crustal minerals gypsum and pyrite. Additional S is found dissolved in ocean water. Thus, with respect to pools, the global S cycle resembles the global cycle of phosphorus (Chapter 12). In contrast, the largest pool of the global N cycle is found in the atmosphere.

In other respects, however, there are strong similarities between the global cycles of N, S, and Hg. In all cases, the major annual movement of the element is through the atmosphere, and under natural conditions a large portion of the movement is through the production of reduced gases by biological activity. These gases return N, S, and Hg to the atmosphere, providing a closed global cycle with a relatively rapid turnover. In contrast, the ultimate fate for P is incorporation into ocean sediments, where the cycle of P is complete only as a result of long-term sedimentary uplift.

Biogeochemistry exerts a major influence on the global S cycle. The largest pool of S near the surface of the Earth is found in sedimentary pyrite, as a result of sulfate reduction. The sedimentary record shows that the relative extent of sulfate reduction has varied through geologic time. In the absence of sulfate-reducing bacteria, the concentration of SO_4^{2-} in seawater would be higher and O_2 in the atmosphere would be lower than present-day values (Eq. 9.2).

Current human perturbations of the sulfur and mercury cycles are extreme—roughly doubling the annual mobilization of these elements from the crust of the Earth. As a result of fossil fuel combustion, areas that are downwind of industrial regions now receive massive amounts of acidic deposition and mercury from the atmosphere. The excess acidity is likely to lead to changes in rock weathering (Chapter 4), forest growth (Chapter 6), and ocean productivity (Chapter 9). The deposition of mercury in aquatic ecosystems often leads to health advisories for fish consumption.

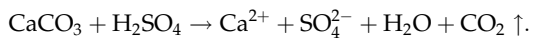
Recommended Reading

- Amend, J.P., K.J. Edwards, and T.W. Lyons (Eds.). 2004. *Sulfur Biogeochemistry: Past and Present*. Geological Society of America.
- Brimblecombe, P., and A.Y. Lein (Eds.). 1989. *Evolution of the Global Biogeochemical Sulphur Cycle*. Wiley.
- Howarth, R.W., J.W.B. Stewart, and M.V. Ivanov (Eds.). 1992. *Sulphur Cycling on the Continents*. Wiley.
- Ivanov, M.V., and J.R. Freney (Eds.). 1983. *The Global Biogeochemical Sulfur Cycle*. Wiley.

PROBLEMS

1. Today, there is approximately 3750×10^{18} g S found as sulfate in seawater and evaporite deposits. Assuming that this sulfur was originally delivered to the oceans in the form of sulfides emitted from hydrothermal emissions, how long would the oxidation of sulfides provide a sink for oxygen derived from the earliest photosynthetic organisms? (Assume that the net storage of organic carbon in sediments of the Precambrian ocean is roughly similar to that of today— 0.1×10^{15} g C/yr.)
2. Volcanic gases contain Hg/CO_2 and $\text{Hg}/\text{H}_2\text{O}$ in a ratio of 10^{-8} (Engle et al. 2006) and in a ratio of 10^{-5} with SO_2 (Bagnato et al. 2011). Calculate a global estimate of Hg emission from volcanoes that derives from the global cycles of C, H_2O , and S, as presented in this book.

3. When acid rain falls on carbonate-rich soils, CO₂ is released in the following reaction:



Provide a quantitative estimate of the maximum potential importance of this as a source of atmospheric CO₂ versus that derived directly from fossil fuel combustion.
